

Hydrogen local modes and shallow donors in ZnO

G. Alvin Shi and Michael Stavola

Department of Physics, Lehigh University, Bethlehem, Pennsylvania 18015, USA

S. J. Pearton

Department of Materials Science and Engineering, University of Florida, Gainesville, Florida 32611, USA

M. Thieme, E. V. Lavrov, and J. Weber

Institut für Angewandte Physik, Technische Universität Dresden, D-01062 Dresden, Germany

(Received 29 August 2005; revised manuscript received 29 September 2005; published 28 November 2005)

The annealing behavior of the free-carrier absorption, O-H vibrational absorption, and photoluminescence lines previously associated with H-related donors in ZnO has been studied. One set of H-related defects gives rise to O-H local vibrational mode absorption at either 3326 or 3611 cm^{-1} , with the relative intensities of these lines depending on the source of the ZnO starting material. These O-H lines anneal away together at 150 °C along with $\sim 80\%$ of the free carriers introduced by H. The common annealing behavior of the O-H ir lines suggests that they are closely related. An additional defect produced by hydrogenation is thermally stable up to an annealing temperature of 500 °C where a bound-exciton photoluminescence line often associated with H in ZnO is also annealed away. This more thermally stable donor accounts for $\sim 20\%$ of the free carriers introduced by H. These experiments on H in ZnO reveal a complex behavior with several defects being introduced and with properties that depend strongly on the source of the ZnO starting material.

DOI: [10.1103/PhysRevB.72.195211](https://doi.org/10.1103/PhysRevB.72.195211)

PACS number(s): 61.72.Cc, 63.20.Pw, 78.30.Fs

I. INTRODUCTION

ZnO is a wide-band-gap semiconductor that has attracted much recent interest because of its possible application in optoelectronic devices.^{1,2} ZnO can be grown by a variety of methods and is typically *n* type. To explain the *n*-type conductivity of ZnO, Van de Walle proposed that H impurities are introduced unintentionally into ZnO during crystal growth, and that H acts as a shallow donor instead of passivating dopants as is usually the case for H in semiconductors.³ Several possible configurations for H⁺ in ZnO in which a strong O-H bond is formed were found to have similar formation energies, and the complex of H with an oxygen vacancy was also found to be a shallow donor.³ While several additional defects and impurities in ZnO can also give rise to shallow donors,^{1,2,4} H is especially important because it can be introduced easily during crystal growth and device processing.⁵

Hydrogen's role as a shallow donor in ZnO was explored in early experimental studies performed in the 1950s.⁶⁻⁹ The introduction of H from a H₂ ambient was found to increase the *n*-type conductivity of ZnO, and the solubility and diffusivity of H in ZnO were determined. In recent studies of H's role as a shallow donor in ZnO, a variety of experimental probes has been used that include muon spin resonance (μSR),¹⁰ electron paramagnetic resonance, electron nuclear double resonance (ENDOR),¹¹ photoluminescence (PL),^{4,12} and local vibrational mode (LVM) spectroscopy.¹³⁻¹⁵ These experiments have often been performed in conjunction with Hall-effect measurements that probe the concentration of free carriers. A common conclusion of these experiments is that H forms a shallow donor in ZnO.

Spectroscopic signatures that have been associated with H in ZnO are a bound-exciton luminescence line known as *I*₄

and O-H LVM lines at 3611 and 3326 cm^{-1} . The *I*₄ PL line has frequently been observed in as-grown ZnO samples and in samples hydrogenated from a hydrogen plasma.^{4,12} An O-H vibrational line at 3611 cm^{-1} , with a transition moment oriented along the *c* axis, was discovered by Lavrov *et al.* for ZnO samples treated in a hydrogen plasma.¹⁴ The 3611 cm^{-1} line was assigned to a center containing an O-H bond aligned along the *c* axis of the crystal. A different O-H vibrational line at 3326 cm^{-1} was discovered by McCluskey *et al.* for ZnO samples annealed in H₂ gas at elevated temperature ($\sim 700^\circ\text{C}$),¹⁵ making contact with the studies of H in ZnO performed in the 1950s.⁶⁻⁹ The 3326 cm^{-1} line was assigned to an O-H center with a transition moment oriented at an angle of 112° with respect to the *c* axis.¹⁶ Additional H-related LVMs have been reported,¹³⁻¹⁵ including a strong ir line at 3577 cm^{-1} that has been assigned to a Li-H center found in hydrothermally grown ZnO.^{17,18}

While a variety of results confirm that H is a shallow donor in ZnO, the experimental data for H in ZnO remain puzzling and suggest that the situation is more complicated than there being a single shallow-donor species associated with H. There are two different O-H LVMs with each of the ir lines being seen by different groups in ZnO samples grown and hydrogenated by different methods.¹⁴⁻¹⁶ Furthermore, the *I*₄ bound-exciton line seen with PL is found in as-grown ZnO samples and is stable upon annealing up to temperatures near 500 °C.^{4,12} The 3326 and 3611 cm^{-1} LVM lines have been found to be unstable for thermal annealing at considerably lower temperatures.^{14,16,19,20} The differences in the annealing behaviors associated with the different spectroscopic signatures make it unlikely that only one H-related defect is being observed by the different experimental methods.²¹ Furthermore, there have been a few calibrations that relate the intensity of the 3326 cm^{-1} ir line to the free-carrier concen-

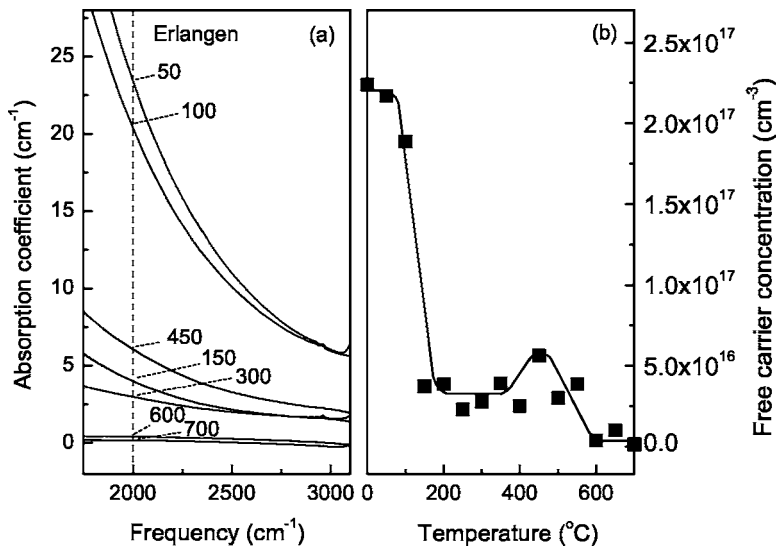


FIG. 1. (a) Free-carrier absorption spectra (room temperature, resolution 2 cm^{-1}) for a ZnO sample obtained from the University of Erlangen. The sample was first annealed (30 min) at 725 $^{\circ}\text{C}$ in H_2 gas to introduce H. The sample was subsequently annealed in a He ambient at the temperatures shown (in $^{\circ}\text{C}$). Anneals were terminated by a quench to room temperature. The reference spectrum for these data (not shown) was measured for the same sample following an anneal at 750 $^{\circ}\text{C}$ in a He ambient that was performed to remove H. (b) Free-carrier concentration [determined from the absorption coefficient at 2000 cm^{-1} in (a)] vs annealing temperature.

tration in ZnO, and these calibrations vary by a factor of ~ 50 (Refs. 15, 19, and 20). These various disjointed and sometimes contradictory results make uncertain the relationship of the H donors produced by the intentional introduction of H into ZnO as was first explored in the 1950s to the shallow donors found in modern, as-grown samples. It is also uncertain how the various spectroscopic signatures commonly associated with H are related to these donor defects and to each other.

In the present paper, the LVM signatures at 3326 and 3611 cm^{-1} previously associated with O-H centers in ZnO (Refs. 14 and 15) are studied for samples grown by a variety of methods. H was introduced into all of these samples by annealing in H_2 gas, and the annealing behavior of the O-H ir lines along with the concentrations of free carriers in the samples has been studied. These results are also compared with the annealing behavior of the I_4 PL line that has been associated with a shallow H donor. These results help to clarify the relationship between the H-related defects seen in various studies and the free carriers that are produced by the introduction of H.

II. EXPERIMENT

ZnO samples for our experiments were obtained from a variety of sources. Samples grown by seeded chemical vapor transport were obtained from Eagle Picher.²² Melt-grown ZnO samples were purchased from Cermet, Inc.²³ A few samples were prepared from hexagonal ZnO prisms grown from the vapor phase at the University of Erlangen, Germany.²⁴ (We also examined ZnO samples that had been hydrothermally grown, but these were dominated by a Li-H complex^{17,18} that is not of interest in the present paper.) To introduce H, ZnO samples were placed in sealed quartz ampoules filled with H_2 gas ($2/3$ atm at room temperature), annealed at 725 $^{\circ}\text{C}$, and quenched to room temperature in water to terminate the anneals. Subsequent anneals were performed in an inert gas ambient, either He or Ar.

Samples were prepared from the hexagonal prisms grown at the University of Erlangen²⁴ with a $\{10\bar{1}0\}$ face so that the

c axis was parallel to one of the edges of the sample. For samples oriented in this way, a defect with a transition moment along the c direction could be readily studied. Our other samples were prepared from c -cut wafers. For a light beam at normal incidence, the polarization with $\mathbf{E} \parallel \mathbf{c}$ could not be explored. For several of our experiments, samples were rotated so that the probing light was incident at a 45 $^{\circ}$ angle with respect to the c axis. In this way, O-H centers with transition moments parallel to the c axis could also be investigated for the c -cut wafers.

ir absorption spectra were measured with a Bomem DA.3 Fourier transform infrared spectrometer. H vibrational modes were measured in ZnO samples at 4.2 K with an InSb detector. The absorption due to free carriers was measured in ZnO samples at room temperature with a HgCdTd detector. (Free-carrier absorption in ZnO was studied in early work by Thomas⁹ and provides a contact-free method to probe the free-carrier concentration that is particularly convenient for annealing experiments.) For PL measurements, a ZnO sample was immersed in liquid He at 4.2 K. The sample was excited with the 325 nm line of a HeCd laser with a typical excitation power of 8 mW. The emitted light was dispersed by a single-grating monochromator with a spectral resolution of 0.025 nm. Spectra were measured for several different positions to ensure that the results were representative of the whole sample.

III. EXPERIMENTAL RESULTS

A. Free-carrier absorption and its decay upon annealing

Figure 1(a) shows the broad ir absorption that is due to the free carriers that are introduced into ZnO by a hydrogenation treatment. For this experiment, a ZnO sample prepared from a hexagonal prism grown at the University of Erlangen was first annealed in an inert gas ambient at 750 $^{\circ}\text{C}$ for 30 min to outdiffuse any H that might have been present in the as-grown sample. We have found that such an anneal is sufficient to eliminate the free carriers and the ir and PL lines attributed to H. Hydrogen was then introduced intentionally into the sample by an anneal at 725 $^{\circ}\text{C}$ (30 min) in a

sealed ampoule that contained H_2 gas. This anneal was terminated by quenching the ampoule in water to room temperature. The surfaces of the samples were repolished following the anneals in H_2 . The samples from other suppliers also showed an increase in the absorption due to free carriers following hydrogenation.

The strongest free-carrier absorption is seen after the introduction of H and is then reduced in spectra that were measured following a series of anneals performed in an inert ambient. To produce the series of free-carrier absorption spectra that is shown in Fig. 1, a reference spectrum was measured for the same sample following an anneal at 750°C in a He ambient that was performed to remove H. This reference spectrum was subtracted from all of the spectra that were measured following anneals performed at lower temperatures. With the reference spectrum chosen in this way, the free carrier absorption that is shown in Fig. 1 is that which is due to carriers that are related to H in the sample. The absorption coefficient at a given frequency is proportional to the concentration of free electrons in the sample.⁹ The absorption coefficient at 2000 cm^{-1} was calibrated in a previous study by Hall measurements,¹⁹ and this calibration has been used here to determine the concentration of free carriers that was present following each annealing step.²⁵

Figure 1(b) shows the concentration of free carriers vs the annealing temperature. We note that the ampoule containing the ZnO sample was quenched to room temperature in water to terminate each anneal. As the annealing temperature is increased, 80% of the free carriers are removed by the annealing step near 150°C . Upon a further increase in the annealing temperature, a fraction ($\sim 10\%$) of the free carriers is recovered near 450°C . This partial recovery of the free-carrier absorption occurs only for samples that are rapidly quenched following annealing. For samples that are slowly cooled, the free-carrier absorption remains unchanged from its value following the 150°C anneal (see Fig. 3 in Ref. 19) up to temperatures near 500°C . Annealing at temperatures above 500°C results in a removal of the remaining free carriers due to H, i.e., the $\sim 20\%$ of the free-carrier absorption that remained after the anneal at 150°C .

A similar series of anneals and ir measurements of the free-carrier absorption was performed for a ZnO sample obtained from Eagle Picher that had been hydrogenated by an anneal at 725°C (30 min) in H_2 gas. An annealing curve similar to the one shown in Fig. 1(b) was obtained in which $\sim 80\%$ of the H-related, free-carrier absorption was eliminated by an anneal near 150°C and with the remaining 20% being eliminated for an anneal near 500°C . (The results of a similar experiment performed previously for a sample obtained from Eagle Picher were reported in Ref. 19.)

B. O-H local mode absorption and its annealing behavior

Figure 2 shows low-temperature ir results for ZnO samples obtained from different sources. These samples were hydrogenated by an anneal in H_2 gas at 725°C , similar to the sample whose free-carrier absorption spectra are shown in Fig. 1. The absorption coefficients for the polarizations of the incident light with $\mathbf{E}\parallel\mathbf{c}$ and $\mathbf{E}\perp\mathbf{c}$ were determined directly

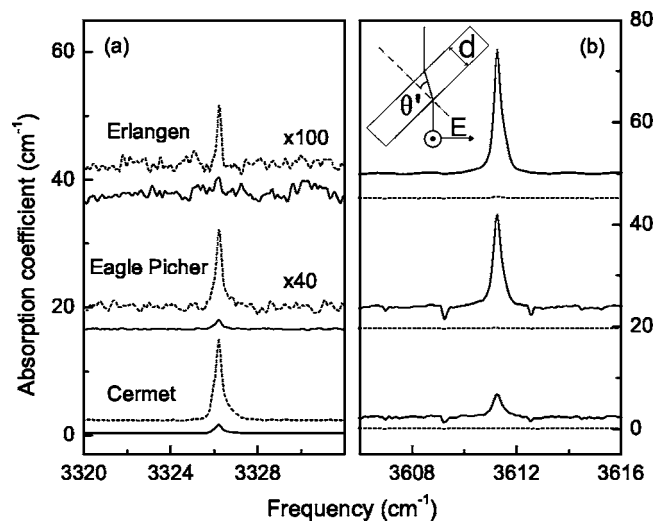


FIG. 2. ir absorption spectra ($T=4.2\text{ K}$, resolution= 0.15 cm^{-1}) for ZnO samples obtained from different suppliers. The spectra for the different polarizations were determined directly for the sample obtained from the University of Erlangen with a $\{10\bar{1}0\}$ face. The spectra for the samples obtained from Eagle Picher and Cermet were determined from polarization data for a c -cut sample tilted at 45° with respect to the viewing axis (see inset). (Spectra with $\mathbf{E}\parallel\mathbf{c}$ are shown by —, and with $\mathbf{E}\perp\mathbf{c}$ by ---.)

for the sample with a $\{10\bar{1}0\}$ face prepared from the hexagonal prisms grown at the University of Erlangen. For the c -cut samples obtained from the other suppliers, the absorption coefficients for the different polarizations were determined from spectra measured with polarized light for a sample turned at a 45° angle with respect to the optical viewing axis (see the inset in Fig. 2). While the orientations of the transition moments for the different lines could be determined in principle from measurements made for the rotated sample, these orientations have been determined previously for the 3326 and 3611 cm^{-1} lines that are of interest here.^{14,16,20} Taking the 3611 cm^{-1} line as an example, with its transition moment directed along the c axis of the sample,¹⁴ the spectrum measured with $\mathbf{E}\perp\mathbf{c}$ (with the polarization normal to the page for the inset in Fig. 2) shows no absorption at 3611 cm^{-1} , confirming that the transition moment is oriented along the c axis. For the polarization oriented at an angle with respect to the sample surface, the absorption coefficient for $\mathbf{E}\parallel\mathbf{c}$, $\alpha_{\parallel}(3611)$, is obtained from the measured absorbance $A(\bar{\nu})$ from the equation

$$\alpha_{\parallel}(3611) = (\cos \theta' / \sin^2 \theta') \ln_{10}[A(\bar{\nu})/x]. \quad (1)$$

Here, θ' is the angle between the propagation direction of the polarized light inside the sample and the c axis, and x is the sample thickness. The absorption coefficients for $\mathbf{E}\parallel\mathbf{c}$ and $\mathbf{E}\perp\mathbf{c}$ for c -cut samples were determined by a similar analysis for the 3326 cm^{-1} line from ir measurements made with the polarization geometry shown in the inset to Fig. 2 and the known direction of its transition moment (112° with respect to the c axis^{16,20}).

The spectra in Fig. 2 show that both the 3326 and 3611 cm^{-1} ir lines seen previously^{14,15} are observed in a va-

TABLE I. Room-temperature Hall data for ZnO samples annealed (30 min) at 700 °C in He.

Sample	N (cm ⁻³)	μ (cm ² /V s)
U. Erlangen	3.9×10^{15}	221
Eagle Picher	2.7×10^{16}	203
Cermet	1.6×10^{17}	152

riety of samples grown by different methods but that the relative intensities of these two O-H lines depend greatly on the source of the ZnO material. Samples prepared from the hexagonal prisms grown at the University of Erlangen show predominantly the 3611 cm⁻¹ line, in agreement with the results of Lavrov *et al.*¹⁴ who studied similar samples. (These samples also show the 3326 cm⁻¹ line, but it is sufficiently weak to have been missed in previous experiments.) The samples prepared from ZnO wafers grown by Cermet show predominantly the 3326 cm⁻¹ line studied by McCluskey and co-workers.^{15,16,20} Hydrogenated samples prepared from ZnO wafers obtained from Eagle Picher also show both lines with the 3611 cm⁻¹ line being dominant in this case. (A sample grown by the hydrothermal method was also examined in these experiments. In this case, neither the 3326 nor 3611 cm⁻¹ lines was produced, and only the 3577 cm⁻¹ line that has been assigned to a Li-H complex^{17,18} was seen following hydrogenation. Presumably, Li impurities effectively trap all of the H introduced into these samples. ZnO grown by the hydrothermal method is not discussed further in this paper.) The spectra in Fig. 2 immediately show that both the 3326 and 3611 cm⁻¹ O-H LVMs are produced by similar hydrogenation treatments and that the source of the ZnO starting material determines which of the O-H lines is seen.

The different samples whose spectra are shown in Fig. 2 have very different background carrier concentrations when H has been removed. Samples from different sources were annealed in He at 750 °C (30 min) to remove H. The concentrations of free carriers were then determined with Hall measurements. Results are shown in Table I. The sample from Cermet had the greatest concentration of background donors, and the sample grown at the University of Erlangen the least, with the concentration of donors differing by a factor of ~40.

Figure 3 shows spectra for the 3326 and 3611 cm⁻¹ ir lines for the same sample and series of anneals as for the free-carrier-absorption data shown in Fig. 1. Figure 4 shows the intensity of the 3611 cm⁻¹ line which was dominant in this sample vs the annealing temperature. The 3326 and 3611 cm⁻¹ lines are eliminated together by an anneal near 150 °C. Both lines are recovered partially when the H-related, free-carrier absorption is recovered partially by an anneal near 450 °C, and both lines disappear together for an anneal above 500 °C. The partial recovery of the 3326 and 3611 cm⁻¹ lines for an anneal near 450 °C occurred only for samples that were quenched to terminate the anneals, similar to the recovery of the free-carrier absorption discussed above. Surprisingly, the 3326 and 3611 cm⁻¹ lines disappear and appear together, and this annealing behavior is correlated with the behavior of the fraction of the free-carrier absorp-

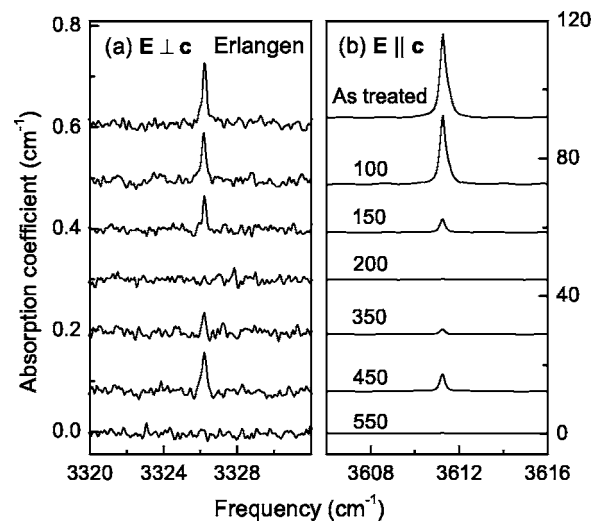


FIG. 3. ir absorption spectra ($T=4.2$ K, resolution= 0.15 cm⁻¹) for a ZnO wafer obtained from the University of Erlangen. (a) shows spectra for the 3326 cm⁻¹ ir line for $E \perp c$, and (b) shows spectra for the 3611 cm⁻¹ ir line for $E \parallel c$. The uppermost spectra were measured after an anneal (30 min) at 725 °C in H₂ gas that was performed to introduce H. Other spectra were measured following anneals (30 min) performed in a He ambient at the temperatures shown (in °C). Anneals were terminated by a quench to room temperature.

tion (80%) that is eliminated by the anneal at 150 °C.

Very similar annealing results were obtained for the O-H ir lines for ZnO samples obtained from Eagle Picher and from Cermet, Inc. The local modes at 3326 and 3611 cm⁻¹ had a different relative intensity in the different samples, as is shown in Fig. 2, but both were eliminated by an anneal near ~150 °C. Recent results by Jokela and McCluskey²⁰ also show that the disappearance of the 3326 cm⁻¹ ir line and H-related free carriers are closely correlated for samples grown by Cermet.

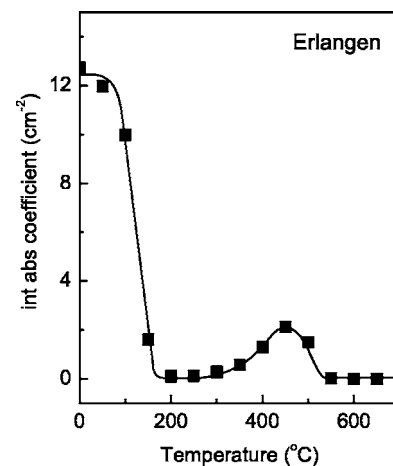


FIG. 4. Integrated area of the 3611 cm⁻¹ ir line vs annealing temperature for a ZnO sample obtained from the University of Erlangen. Selected spectra are shown in Fig. 3. The sample was initially hydrogenated by an anneal in H₂ gas (725 °C, 30 min) followed by an anneal in a He ambient at the indicated temperatures. Anneals were terminated by a quench to room temperature.

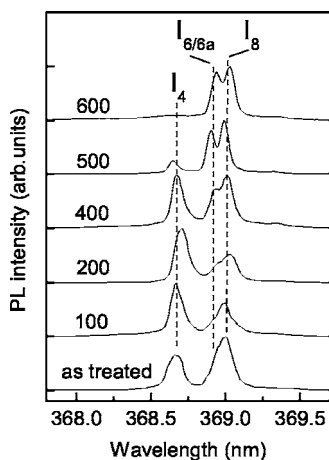


FIG. 5. Photoluminescence spectra (4.2 K) in the bound-exciton range for a ZnO sample obtained from Eagle Picher. The sample was first annealed (30 min) at 725 °C in H₂ gas to introduce H. This anneal was terminated by a quench to room temperature. The sample was subsequently annealed in an Ar ambient (30 min) at the temperatures shown (in °C).

C. Annealing behavior of the I_4 bound-exciton PL line

Figure 5 shows the bound-exciton PL emission lines associated with shallow donors in ZnO.²⁶ These results are for a sample grown by Eagle Picher that was hydrogenated by annealing in H₂ gas at 725 °C followed by a quench to room temperature in a sealed ampoule. The line labeled I_4 that has been attributed to an H-related shallow donor is present.^{4,12} Ir measurements confirmed that strong O-H local mode absorption was also produced by this hydrogenation treatment. This ZnO sample was then annealed (30 min) in an inert ambient at successively higher temperatures. The relative intensity of the I_4 PL line (i.e., the ratio of the I_4 intensity to that of the $I_{6/6a}$ and I_8 lines) changes by only a small factor for annealing temperatures up to 400 °C. For higher annealing temperatures, $T \geq 500$ °C, the intensity of the I_4 line was decreased and then completely eliminated. In particular, there is little change in the relative intensity of the I_4 line near 150 °C where the free-carrier and O-H local mode absorption are strongly affected by annealing. The thermal stability of the I_4 PL line shown in Fig. 5 is consistent with results in the literature obtained by other research groups.^{4,12}

IV. DISCUSSION

A. Relationship between the spectroscopic signatures for H and the annealing of free carriers

Figure 1 shows that the free-carrier concentration that results from a hydrogenation treatment of ZnO decays in two steps. Approximately 80% of the free carriers are removed at the first step near 150 °C. Figures 3 and 4 show that the decay of the O-H LVM absorption lines at both 3326 and 3611 cm⁻¹ is well correlated with this annealing step. A portion of the free carriers and the O-H ir intensity can be regenerated by annealing the sample at higher temperature (~450 °C) and quenching, showing that the hydrogen does not completely leave the sample during the anneal at 150 °C.

Finally, the remaining free carriers (20%) are removed in a second annealing step near 500 °C. Similar annealing behavior has been seen for other samples in other studies.^{16,19,20,27} Figure 5 shows that the decay of the I_4 PL line is correlated with the annealing step at 500 °C. At this point, the free-carrier absorption and O-H local modes can no longer be recovered by quenching the sample, consistent with the diffusion of H out of the sample.

A comparison of the annealing behaviors of the absorption due to free carriers, the O-H LVM lines at 3326 and 3611 cm⁻¹, and the I_4 PL line leads to the conclusion that annealing ZnO in H₂ gas must introduce more than one defect that increases the free-carrier concentration. Furthermore, the annealing data suggest that the defects that give rise to the O-H LVM lines account for ~80% of the H-related free carriers in the sample immediately following hydrogenation and that these O-H centers transform into an electrically inactive species upon annealing at 150 °C. These O-H centers are not likely to give rise to the H donor seen in as-grown ZnO samples in recent studies because they are not stable for prolonged storage times at room temperature. The disappearance of the O-H centers at 150 °C and their ir lines results in the formation of an electrically inactive hydrogen species that recent studies suggest is H₂.^{19,20}

An additional, more thermally stable defect accounts for ~20% of the free carriers introduced by H and is removed by thermal annealing at $T \geq 500$ °C. The annealing data suggest that this is the defect that gives rise to the I_4 PL line. This H-related donor is also likely to be the H-related shallow donor that is typically found in as-grown samples because it has sufficient thermal stability to remain electrically active following sample storage at room temperature for times greater than one month.

Therefore, there are three distinct types of H-related defects that can be produced in ZnO: (i) the O-H centers that give rise to two different LVM absorption lines that anneal away at 150 °C, (ii) the more thermally stable shallow donor that gives the I_4 PL line, and (iii) an electrically inactive form of H, presumably H₂, that is formed by the diffusion of H. It is puzzling that there is no H-related vibrational mode associated with the shallow donor that gives the I_4 bound-exciton line and no bound exciton associated with the defects that give rise to the O-H local vibrational modes. It is possible that the defect giving the I_4 line has a low vibrational frequency and has escaped detection. The O-H ir lines might be associated with deep donors²⁸ that are nonetheless ionized at room temperature or possibly with H-passivated acceptors that increase the concentration of free carriers in the samples through the neutralization of compensating acceptors.

B. O-H local vibrational modes

The O-H LVMs show a complicated and interesting behavior. There are two different O-H structures, with different LVM frequencies and transition moment directions, introduced together by annealing ZnO in H₂ gas. Nonetheless, the 3326 and 3611 cm⁻¹ lines appear and disappear together upon annealing as if the local modes belong to strongly related defects. Which configuration and ir absorption line are

obtained depends strongly on the source of the ZnO starting material. The different ZnO samples studied here have very different background doping levels (Table I), so that which defect is seen might depend on the position of the Fermi level in the sample. The 3326 cm^{-1} line is favored in samples with a higher background conductivity while the 3611 cm^{-1} line is favored in samples with lower conductivity. We recognize that the determination of the Fermi level in the hydrogenated ZnO is complicated because H also introduces free carriers. Nonetheless, the background doping concentration in the samples (Table I) ranges from values comparable to the carrier concentration introduced by H [Fig. 1(b)] to values that are much less, so that the concentration of background donors will have an important effect on the charge states of defects in the samples. While it is tempting to associate the intensities of the 3326 and 3611 cm^{-1} lines with a shift in the Fermi level for the different samples we must also be cautious. The difference in the background conductivity of the samples from different sources also implies a different defect and impurity content, and which O-H line is seen may depend simply on the concentrations of the different traps for H in the different samples.

It is puzzling that the two different O-H defect structures show closely similar annealing behavior. One possible model is that both structures are formed as a sample is cooled to low temperature from one H defect that is present at an elevated temperature (that must be below $150\text{ }^\circ\text{C}$ where the O-H ir lines are annealed away). The properties of this H defect would determine the annealing behavior that occurs at elevated temperature for both ir lines. It is possible that one (or both) of the defects that gives rise to the 3326 and 3611 cm^{-1} ir lines could involve a close pair of H with another defect or impurity. The possibility for H to be trapped by defects is demonstrated by the formation of Li-H complexes in ZnO samples grown by the hydrothermal method.^{17,18,29} An alternative possibility is that a large lattice relaxation (i.e., a bonding rearrangement) that depends on the charge state of the O-H defect occurs, giving rise to O-H configurations with different orientations in the ZnO lattice at the temperature where the ir spectrum is measured.

Secondary illumination has been used to probe the effect that a change in charge state might have on the relative intensities of the 3326 and 3611 cm^{-1} ir lines. Figure 6 shows the effect of illumination at low temperature by white light from a tungsten light source on the O-H ir lines at 3326 and 3611 cm^{-1} . Secondary illumination reduced the intensity of the 3326 cm^{-1} line by a factor greater than 2 for a sample in which the 3611 cm^{-1} line was dominant (obtained from Eagle Picher) and also for a sample for which the 3326 cm^{-1} line was dominant (obtained from Cermet). However, there is no complementary change in the intensity of the 3611 cm^{-1} line seen for either sample. Up to this point, we have been vague about whether the defect structures giving rise to the O-H ir lines are due to two different defects or to two different configurations of the same defect. The effect of secondary illumination suggests that two different defects are being seen at low temperature, one that is sensitive to illumination and one that is not, and that the 3326 and 3611 cm^{-1} lines are not associated with different charge states of the same defect because *complementary* changes in

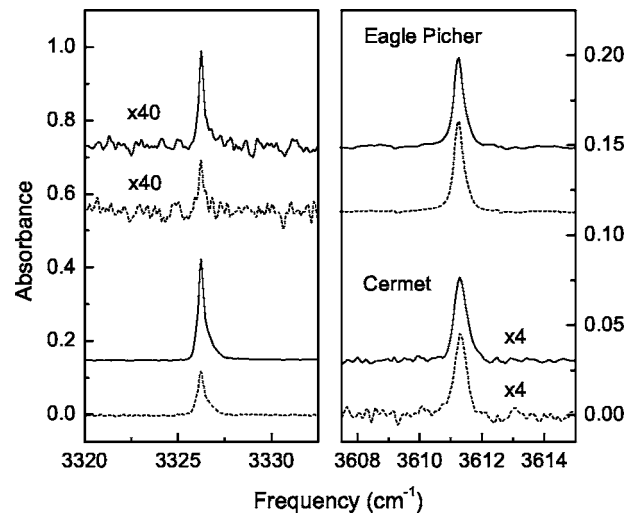


FIG. 6. ir absorption spectra ($T=4.2\text{ K}$, resolution= 0.15 cm^{-1}) for c -cut ZnO wafers obtained from Eagle Picher (upper spectra) and Cermet (lower spectra). The samples were first annealed (30 min) at $725\text{ }^\circ\text{C}$ in H_2 gas to introduce H. The samples were rotated so that the probing light (unpolarized) was incident at 45° with respect to the c axis so that defects with transition moments parallel or perpendicular to the c axis could be observed. The sample was illuminated during the ir measurement at 4.2 K from the side by the white light from a tungsten light source for two of the spectra shown. (Spectra without secondary illumination are shown by —, and with secondary illumination by ---.)

intensity do not occur upon illumination. The reduction in intensity of the 3326 cm^{-1} ir line upon illumination may be due to a change in frequency of the mode and possibly absorption strength that occurs upon a change of charge state.³⁰ Additional experiments are in progress to further investigate the defect configurations giving rise to the 3326 and 3611 cm^{-1} O-H LVMs and their relationship to each other.

Our results show that H in ZnO can form different defects that increase the free-carrier concentration. Furthermore, which spectroscopic signatures occur depends on the source of the ZnO starting material. Therefore, it is difficult to relate the concentration of free carriers to, say, the intensity of one of the O-H LVMs that has been observed. This situation explains why greatly different results have been found in experiments that attempt to relate the O-H ir intensity for the 3326 cm^{-1} line to the concentration of free carriers.^{15,19,20}

C. Evolution of H-containing centers upon annealing

The explanation of the annealing behavior of the H-related, free-carrier absorption and the O-H ir lines at 3326 and 3611 cm^{-1} follows that proposed in Ref. 19. H that is introduced by annealing ZnO in H_2 gas at elevated temperature becomes frozen into electrically active defects upon quenching. There are two different O-H configurations that give rise to O-H vibrational lines. When the sample is annealed near $150\text{ }^\circ\text{C}$, the H does not yet leave the sample but diffuses to form electrically inactive H_2 defects that are more stable than the O-H defects frozen in by quenching. This suggestion is strongly supported by the recent results of a

study by Jokela and McCluskey who find that the kinetics of the decay of the hydrogen-related free carriers and O-H ir intensity follow a bimolecular decay model that is consistent with the diffusion of H to form H_2 .²⁰ Subsequent annealing near 400 °C dissociates the H_2 , and the liberated H can once again form the electrically active O-H defects that become frozen in if the sample is quenched to terminate the anneals. Prolonged annealing at 400 °C and higher temperatures dissociates all of the H_2 molecules and the liberated H finally diffuses out of the samples. The elimination of the remaining 20% of the free-carrier absorption that occurs for an annealing temperature above ~ 500 °C is due to the removal of an additional, more thermally stable shallow donor defect in the ZnO that is also produced by the hydrogenation treatment.

V. CONCLUSION

In conclusion, a number of groups, beginning in the 1950s, have recognized that the introduction of H into ZnO produces H-related donors.^{3,4,6-15} Our results for the annealing behavior of the free-carrier absorption, O-H ir absorption, and I_4 PL signatures previously associated with H-related donors show that annealing ZnO in H_2 gas introduces more than one defect that gives rise to free carriers.

One set of H-related defects gives rise to O-H local mode absorption at either 3326 or 3611 cm^{-1} , with the relative intensities of these lines depending on the source of the ZnO starting material. The O-H local mode absorption of both of these lines decays upon annealing near 150 °C where $\sim 80\%$ of the H-related, free-carrier absorption is also eliminated. At this temperature, H does not leave the bulk of the sample during a 30 min anneal, but instead forms an inactive species that has been suggested to be H_2 .^{19,20}

An additional defect produced by hydrogenation is thermally stable up to an annealing temperature of 500 °C. At this temperature H can diffuse out of the sample, and the remaining free-carrier absorption ($\sim 20\%$) is eliminated together with the I_4 bound-exciton PL line. It is this more thermally stable defect that is likely to be the H-related donor that is commonly seen in as-grown samples that have been stored at room temperature.

The annealing data presented here show that a ZnO crystal that is grown or processed in an H-containing ambient and slowly cooled rather than quenched (or stored for a prolonged time) will contain the more thermally stable shallow donor that gives rise to the I_4 PL line and that this defect will dominate the H-related conductivity. A large concentration of electrically inactive H_2 can also be formed by the diffusion of H as the crystal is cooled. This electrically inactive H_2 can be dissociated by thermal annealing near 450 °C and quenching, making possible surprising changes in the conductivity of annealed ZnO samples.¹⁹

Experiments on H in ZnO reveal an especially complex behavior with several defects being introduced and with properties that depend strongly on the source of the ZnO starting material. An explanation of the fascinating properties of these H-related defects remains as a challenge. While we have focused on H-related centers produced in nominally undoped ZnO by annealing in H_2 gas that affect the free-carrier concentration, we note that these are not all of the H-related centers that have been seen.^{13,14,17,18} It is no wonder that the results of studies of H in ZnO performed in different laboratories up to now show puzzling inconsistencies. With several different H-related defects and some of the important sources of variability now revealed, it is hoped that it will be possible for the behavior of H in ZnO to be better understood and controlled.

ACKNOWLEDGMENTS

We are grateful to G. D. Watkins and W. B. Fowler for numerous helpful discussions and to M. McCluskey and S. Jokela for discussions and preprints of their work. We also gratefully acknowledge R. Helbig for supplying the ZnO samples grown at the University of Erlangen. Work performed at LU was supported by NSF Grant No. DMR 0403641. The work at UF is partially supported by AFOSR grant under Grant No. F49620-03-1-0370, by the Army Research Office under Grant No. DAAD19-01-1-0603, and the National Science Foundation by Grant No. DMR 0400416 (Dr. L. Hess). M.S. also thanks the Humboldt Foundation for their support of his work in Dresden.

¹D. C. Look, B. Claffin, Ya. I. Alivov, and S. J. Park, *Phys. Status Solidi A* **201**, 2203 (2004).

²S. J. Pearton, D. P. Norton, K. Ip, Y. W. Heo, and T. Steiner, *Prog. Mater. Sci.* **50**, 293 (2005).

³C. G. Van de Walle, *Phys. Rev. Lett.* **85**, 1012 (2000).

⁴B. K. Meyer, H. Alves, D. M. Hoffman, W. Kriegseis, D. Forster, F. Bertram, J. Christen, A. Hoffmann, M. Strassburg, M. D. Worzak, U. Haboek, and A. V. Rodina, *Phys. Status Solidi B* **241**, 231 (2004).

⁵S. J. Pearton, J. W. Corbett, and M. Stavola, *Hydrogen in Crystalline Semiconductors* (Springer-Verlag, Heidelberg, 1992).

⁶E. Mollwo, *Z. Phys.* **138**, 478 (1954); G. Heiland, E. Mollwo, and F. Stöckman, in *Solid State Physics*, edited by F. Seitz and D. Turnbull (Academic Press, New York, 1959), Vol. 8, p. 193.

⁷D. G. Thomas and J. J. Lander, *J. Chem. Phys.* **25**, 1136 (1956).

⁸A. R. Hutson, *Phys. Rev.* **108**, 222 (1957).

⁹D. G. Thomas, *J. Phys. Chem. Solids* **10**, 47 (1959).

¹⁰S. F. J. Cox, E. A. Davis, S. P. Cottrell, P. J. C. King, J. S. Lord, J. M. Gil, H. V. Alberto, R. C. Vilão, J. Piroto Duarte, N. Ayres de Campos, A. Weidinger, R. L. Lichti, and S. J. C. Irvine, *Phys. Rev. Lett.* **86**, 2601 (2001).

¹¹D. M. Hofmann, A. Hofstaetter, F. Leiter, H. Zhou, F. Henecker, B. K. Meyer, S. B. Orlinskii, J. Schmidt, and P. G. Baranov, *Phys. Rev. Lett.* **88**, 045504 (2002).

¹²Y. M. Strzhemechny, H. L. Mosbacher, D. C. Look, D. C. Reynolds, C. W. Litton, N. Y. Garces, N. C. Giles, L. E. Halliburton, S. Niki, and L. J. Brillson, *Appl. Phys. Lett.* **84**, 2545 (2004).

¹³C. H. Seager and S. M. Myers, *J. Appl. Phys.* **94**, 2888 (2003).

- ¹⁴E. V. Lavrov, J. Weber, F. Börrnert, C. G. Van de Walle, and R. Helbig, *Phys. Rev. B* **66**, 165205 (2002).
- ¹⁵M. D. McCluskey, S. J. Jokela, K. K. Zhuravlev, P. J. Simpson, and K. G. Lynn, *Appl. Phys. Lett.* **81**, 3807 (2002).
- ¹⁶S. J. Jokela, M. D. McCluskey, and K. G. Lynn, *Physica B* **340-342**, 221 (2003).
- ¹⁷L. E. Halliburton, L. Wang, L. Bai, N. Y. Garces, N. C. Giles, M. J. Callahan, and B. Wang, *J. Appl. Phys.* **96**, 7168 (2004).
- ¹⁸E. V. Lavrov, F. Börrnert, and J. Weber, *Phys. Rev. B* **71**, 035205 (2005).
- ¹⁹G. A. Shi, M. Saboktakin, M. Stavola, and S. J. Pearton, *Appl. Phys. Lett.* **85**, 5601 (2004).
- ²⁰S. J. Jokela and M. D. McCluskey, *Phys. Rev. B* **72**, 113201 (2005).
- ²¹The hyperfine parameters found in μ SR and ENDOR studies, when scaled for the different magnetic moments of the muon and proton, are different, suggesting that both experiments might not be observing the same defect. G. D. Watkins (private communication).
- ²²D. C. Look, D. C. Reynolds, J. R. Sizelove, R. L. Jones, C. W. Litton, G. Cantwell, and W. C. Harsch, *Solid State Commun.* **105**, 399 (1998).
- ²³D. C. Reynolds, C. W. Litton, D. C. Look, J. E. Hoelscher, B. Claffin, T. C. Collins, J. Nause, and B. Nemeth, *J. Appl. Phys.* **95**, 4802 (2004).
- ²⁴R. Helbig, *J. Cryst. Growth* **15**, 25 (1972).
- ²⁵Our calibration (Ref. 19) of the free-carrier absorption [$n_{fc}=9.3 \times 10^{15} \text{ cm}^{-2} \times \alpha_{fc}(2000 \text{ cm}^{-1})$ in a sample with mobility $169 \text{ cm}^2/\text{V s}$] differs from the early calibration of Thomas by a factor of near 2, similar to recent results of Seager and Myers (Ref. 13).
- ²⁶The frequency scale in Fig. 5 was calibrated with the frequency of the ZnO I_8 luminescence line seen in the spectrum measured following an anneal at 600°C in an inert ambient (Fig. 5) where the PL lines are sharpest. This calibration required that the measured spectra all be shifted by 0.43 nm to longer wavelength to produce the results shown in Fig. 5. With this shift, the wavelengths of the I_4 , $I_{6/6a}$, and I_8 PL lines in all of the PL spectra are in excellent agreement with previous results (Refs. 4 and 12).
- ²⁷Recent results by Jokela and McCluskey (Ref. 20) show that the introduction of H into ZnO grown by Cermet introduces a donor that decays at room temperature (on the time scale of one month) along with the ir line at 3326 cm^{-1} , and that a fraction of the electrical activity produced by H persists ($\sim 10\%$ in these experiments) after the 3326 cm^{-1} line has been annealed away, consistent with the presence of a more thermally stable donor introduced by H.
- ²⁸Recent results suggest that the defect giving rise to the 3611 cm^{-1} ir line might be a deep donor. See E. V. Lavrov, F. Börrnert, and J. Weber, *Phys. Rev. B* **72**, 085212 (2005).
- ²⁹The tendency of H to be trapped by other impurities is also suggested by theory. See M. G. Wardle, J. P. Goss, and P. R. Briddon, *Phys. Rev. B* **71**, 155205 (2005); *Physica B* (to be published).
- ³⁰The disappearance of the 3326 cm^{-1} line upon illumination suggests another interesting possibility for the similar annealing behavior of the 3326 and 3611 cm^{-1} lines. When the intensity of the 3611 cm^{-1} line and the H-related free-electron concentration are reduced by annealing near 150°C , the resulting shift in the Fermi level position may change the charge state of the defect giving rise to the 3326 cm^{-1} line, causing the ir line intensity to be reduced, similar to the reduction in intensity caused by illumination. At present, our understanding of the detailed electrical properties of the ZnO samples obtained from different suppliers is limited, and explanations of the unusual properties of the H-containing defects in these samples remain speculative.